NANOSYSTEMS: PHYSICS, CHEMISTRY, MATHEMATICS, 2015, 6 (4), P. 593–604

Nanodisperse oxide compounds of iron formed in the $FeSO_4$ – KOH – H_2O – H_2O_2 system ($4.0 \leq pH \leq 13.0$)

D. A. Zherebtsov[2], V. Sh. Mirasov[2], D. G. Kleschev[2], E. V. Polyakov[1]

[1]Institute of Solid State Chemistry of the Ural Branch of the Russian Academy of Sciences, Ekaterinburg, Russia
[2]South Ural State University (National research university), Chelyabinsk, Russia

zherebtsov_da@yahoo.com, mirasov@gmail.com, dgk1950dgk@mail.ru, rupolyakov@ihim.uran.ru

PACS 68.55.A **DOI 10.17586/2220-8054-2015-6-4-593-604**

The regularities of phase formation during oxidation of aqueous solutions of $FeSO_4$ and (or) suspensions of $Fe(OH)_2$ at quasi-constant temperature and pH values have been studied for wide intervals of temperature (20 – 85 °C) and (4.0 – 13.0) of the reaction medium. The produced nanodisperse materials have been examined by X-ray phase analysis, IR spectroscopy, scanning electron microscopy and X-ray fluorescence analysis, as well as by thermogravimetric analysis combined with thermal analysis and mass spectrometric analysis of released gases. The dependences of the phase, chemical and disperse compositions of the formed precipitates on the synthesis parameters have been revealed.

Keywords: $FeSO_4$ solutions; $FeOH_2$ suspensions; hydrogen peroxide oxidation; oxide compounds of iron(III).

Received: 2 May 2015

Revised: 13 May 2015

1. Introduction

The oxidation of iron(II) salt solutions and (or) iron(II) hydroxide suspensions leads to the formation of poorly soluble nanodisperse iron(III) compounds exhibiting peculiar and in some cases unique ion-exchange, sorption, magnetic, catalytic and other properties [1–5], attracting much interest of specialists in many different fields. It is established [2, 3, 5–12] that the phase and disperse compositions of these compounds depend on numerous synthetic parameters: the temperature and pH of the reaction medium, concentration of iron(II) ions in solution and of $Fe(OH)_2$ in suspension, the nature of salt anion and alkaline agent cation, the presence of uncontrolled or specially introduced impurities in the solution, as well as the feed rate and activity of oxidizing agent. Until now, the question as to which parameters have a determining influence on the phase and disperse compositions of the formed iron(III) compounds remains a point for debate, which restrains the introduction of advanced technologies for the reproducible preparation of products with optimal functional properties.

The aim of this work is to obtain more accurate information about the regularities of phase formation during the oxidation of aqueous solutions of $FeSO_4$ and (or) suspensions of $Fe(OH)_2$ at quasi-constant values of temperature, total iron(II) concentration in solution (suspension), of reaction medium and average oxidation rate in case the solid solutions K and H_2O_2 are used as alkaline and oxidizing agents, respectively (hereafter the system $FeSO_4$ – H_2O – KOH – H_2O_2).

2. Experimental

The following reagents were used for synthesis: 1.1 M solution of $FeSO_4$ in distilled water, which was preliminarily reduced by iron powder; 3.8 M KOH and 0.9 M H_2O_2 solutions in distilled water. All the reagents were chemically pure. Oxidation was carried out in a 0.5 dm^3 cylindrical reactor furnished with a mixer, electric heating, thermostating, continuous KOH and H_2O_2 solutions dosing and measuring systems.

In all the experiments, the average oxidation rate of iron(II) ions, 15 ± 1 mmol/(dm^3·min), and the total concentration of Fe(II) and Fe(III) in oxidized suspension, 0.51 ± 0.02 mol/dm^3, were maintained constant, while the temperature t and pH were varied. The experiments were performed in the following sequence: the calculated amount of $FeSO_4$ solution was poured into the reactor and heated to preset temperature t (20, 40, 60 or 85 °C); the required pH value of the reaction medium[1] (4.0; 5.5; 6.5; 8.5; 10.5 or 13.0) was achieved by feeding the KOH solution. After that, the H_2O_2 solution was added at a constant rate into the reactor, and in the interval $4.0 \leq \ < 9.0$ the KOH solution was also added to maintain a quasi-constant pH value ($\pm$ 0.25). Note that over time, the temperature of the reaction medium gradually increased by $\Delta t \approx 5$ °C[2] in all the experiments. At the conclusion of oxidation, the precipitate was separated from the mother solution on a Buchner funnel and washed with water until the filtrate contained no sulfate ions; then, it was dried until constant mass at ~ 50 °C and ground.

The obtained samples were examined by X-ray phase analysis (XPA; DRON-3 X-ray unit with digital data recording attachment; filtered $C_{K\alpha}$ radiation; the powder diffraction electronic database ICSD was used). The average size of the precipitate crystals, d, was calculated by the Debye formula from the physical broadening of reflections[3]. The samples obtained at fixed values of $t = 40$ °C ($4.0 \leq$ pH ≤ 13.0) and pH = 6.5 (20 °C $\leq t \leq 85$ °C) were also studied on a scanning electron microscope JEOL JSM-7001F with an energy-dispersion spectrometer Oxford INCA X-max 80 to determine their elemental (X-ray fluorescence spectral analysis – XSA; random error below 5 %) and disperse compositions (scanning electron microscopy – SEM), as well as by thermogravimetric and thermal analysis methods (synchronous analyzer Netzsch STA 449C Jupiter combined with a mass spectrometer Netzsch QMS 403C Aeolos; the thermograms were recorded over 20 – 900 °C at a heating rate of 10 K/min in air flow of 20 ml/min) and IR spectroscopy (Fourier IR spectrometer Bruker Tensor-27; transmission survey in the 400 – 4000 cm^{-1} range in a KBr matrix).

3. Results and discussion

When H_2O_2 is fed into the reactor, a yellow precipitate is formed (experiments at pH = 4.0) or the $Fe(OH)_2$ suspension changes its color (pH $\geq$ 5.5). We note a typical dark-green color of the intermediate samples for suspensions produced at pH 5.5 – 8.5, which changes to yellow, orange or brown at the end of oxidation, depending on the temperature and pH. According to [2, 8], in this pH interval corresponding to partial precipitation of iron(II) ions from the solution, an intermediate compound is formed during oxidation, which is known in the literature as "green rust II". It is this compound which determines the suspension's color.

The XPA data show that the following nanodisperse phases can be formed in the examined system depending on temperature and pH: iron(III) oxyhydroxides of α, γ and δ modifications and iron(III) oxide γ-Fe_2O_3. The phase and disperse compositions of the precipitates,

[1] The time required to attain a preset pH value was less than 3 min.

[2] Hereafter the value of initial temperature t is indicated.

[3] Non-overlapping reflections of phases with crystallographic indices (hkl): α -FeOOH – (110); γ -FeOOH – (120); δ -FeOOH – (101); γ-Fe_2O_3 – (220) were chosen as analytical reflections.

TABLE 1. Phase composition and grain dimension of precipitates as a function of temperature and pH in the system $FeSO_4$ – H_2O – KOH – H_2O_2

pH	Temperature t, °C			
	20	40	60	85
4.0	α(100) 9	α(100) 12	α(100) 19	α(100) 40
5.5	α(40) + γ(60) 8 7	α(80) + γ(20) 12 9	α(95) + γ(5) 18 12	α(5) + γ*(95) – 23
6.5	α(50) + γ(50) 8 7	α(100) 10	α(40) + γ*(60) 12 20	γ*(100) 27
8.5	α(80) + γ(20) 9 10	γ*(100) 20	γ*(100) 23	γ*(100) 30
10.5	α(10) + γ*(90) 10 20	γ*(100) 23	γ*(100) 25	γ*(100) 40
13.0	δ(100) 8	α(40) + δ(60) 10 10	α(40) +δ(60) 15 16	α(45) +γ*(45) + δ(10) 15 50 –

1. α – phase α-FeOOH; γ – phaseγ-FeOOH; δ – phase δ-FeOOH; γ* – phase γ-Fe_2O_3.
2. In the parentheses are depicted mass % of the phase, the numbers under the parentheses mean crystal size, calculated from the X-ray diffraction data, nm.

as functions of oxidation parameters, are presented in Table 1 and Fig. 1, in which the regions of formation of these phases are demonstrated in temperature – coordinates. From Fig. 1, it follows that α-FeOOH is formed over the whole considered pH interval; γ-FeOOH – at $5.5 \leq$ pH < 9.0; δ-FeOOH – at pH ≥ 10.5; and γ-Fe_2O_3 – at 5.5 – 13.0. When the temperature is raised, the pH range in which these phases are formed expand for γ-Fe_2O_3 and α-FeOOH and narrow for γ- and δ-FeOOH. With increased temperature, the reflection half-width $\Delta 2\Theta$ of the corresponding phases decreases, which is indicative of an increase in the average size d of their crystals (Fig. 2).

It follows from the SEM results that each of the synthesized phases has a characteristic crystal morphology, the average size of which depends on the oxidation parameters. In particular, the γ-Fe_2O_3 and δ-FeOOH phases have an isometric (nearly-spherical) crystal shape. The α- and γ-FeOOH crystals are characterized respectively by needle- and plate-like growth forms. Note that the average crystal size determined from the SEM data agrees reasonably well with X-ray analysis data.

The XSA data show that all the synthesized samples consist mainly of iron and oxygen[4], however, they also contain much smaller amounts of potassium and sulfur atoms. The relative contents of Fe/O and S/O in the most typical samples are given in Table 1.

The data for the phase and chemical compositions of the samples are confirmed by the results of IR spectroscopic and thermogravimetric studies. In particular, the IR spectrum of sample 1 (α-FeOOH), which is monophase according to XPA data, contains (Fig. 3, curve a): narrow absorption bands of Fe–O bonds with wave numbers ν 407, 462 and 631 cm^{-1}; vibrations of groups (797 and 893 1787 cm^{-1}); deformation vibrations of H_2O (1645 cm^{-1}), as well

[4]The employed XSA method allows determining the elements with atomic number z $\geq$ 5. Therefore it should be assumed that along with the above mentioned elements, the examined samples contain also hydrogen.

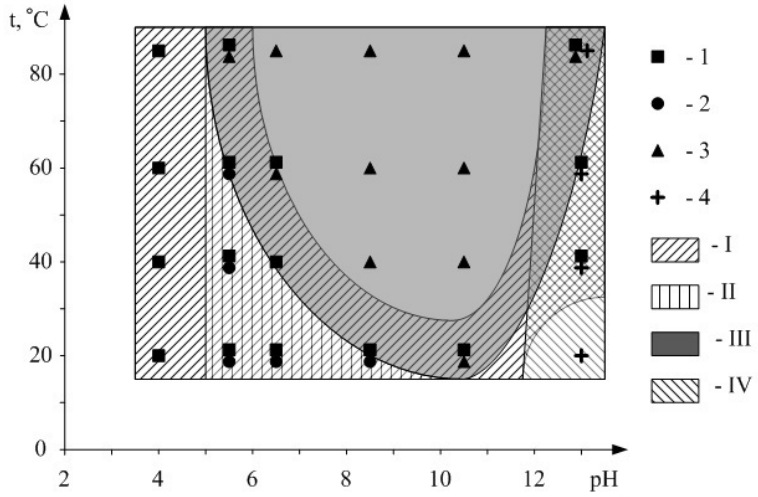

FIG. 1. The phase composition of the precipitate obtained in the system $FeSO_4$ – H_2O – KOH – H_2O_2 as a function of temperature and pH. Designations of phases contained in the precipitate: 1 – α-FeOOH; 2 – γ-FeOOH; 3 – γ-Fe_2O_3; 4 – δ-FeOOH. Phase formation regions: I – α-FeOOH; II – γ-FeOOH; III – γ-Fe_2O_3; IV – δ-FeOOH.

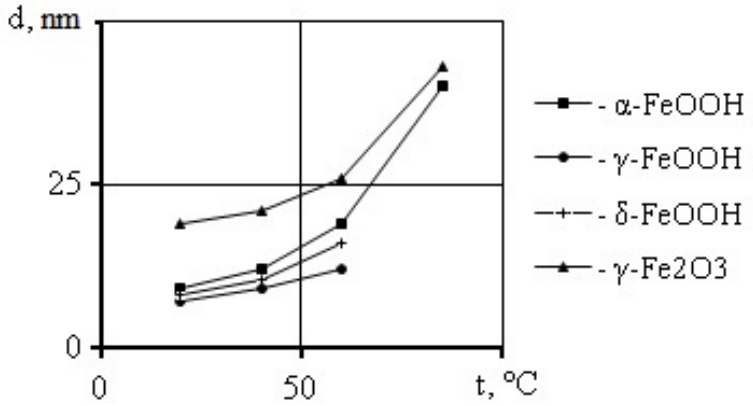

FIG. 2. The average crystal size d (nm) of phases formed in the system $FeSO_4$ – KOH – H_2O – H_2O_2 at a fixed pH value as a function of temperature (t, °C): α-FeOOH (pH – 4.0); γ-FeOOH (pH – 5.5); δ-FeOOH (pH – 13.0); γ-Fe_2O_3 (pH – 10.5).

as a wide absorption band with a maximum at 3158 stretching vibrations of H–O bonds [13]. Additionally, the spectrum of this sample contains weaker absorption bands with ν 1053, 1137 and 1160 cm^{-1}, which can be attributed to the stretching vibrations of $(SO_4)^{2-}$ ions [14].

The IR spectra of the binary mixture samples α- + γ-FeOOH and α- + δ-FeOOH (samples 2 and 4, respectively), along with the absorption bands typical of α-FeOOH, also contain additional absorption bands (Fig. 3, curves b and c) with wave numbers 1022 cm^{-1} (sample 2) and 1050, 1530 cm^{-1} (sample 4). These bands should be attributed to vibrations of groups in γ- and δ-FeOOH, respectively [15].

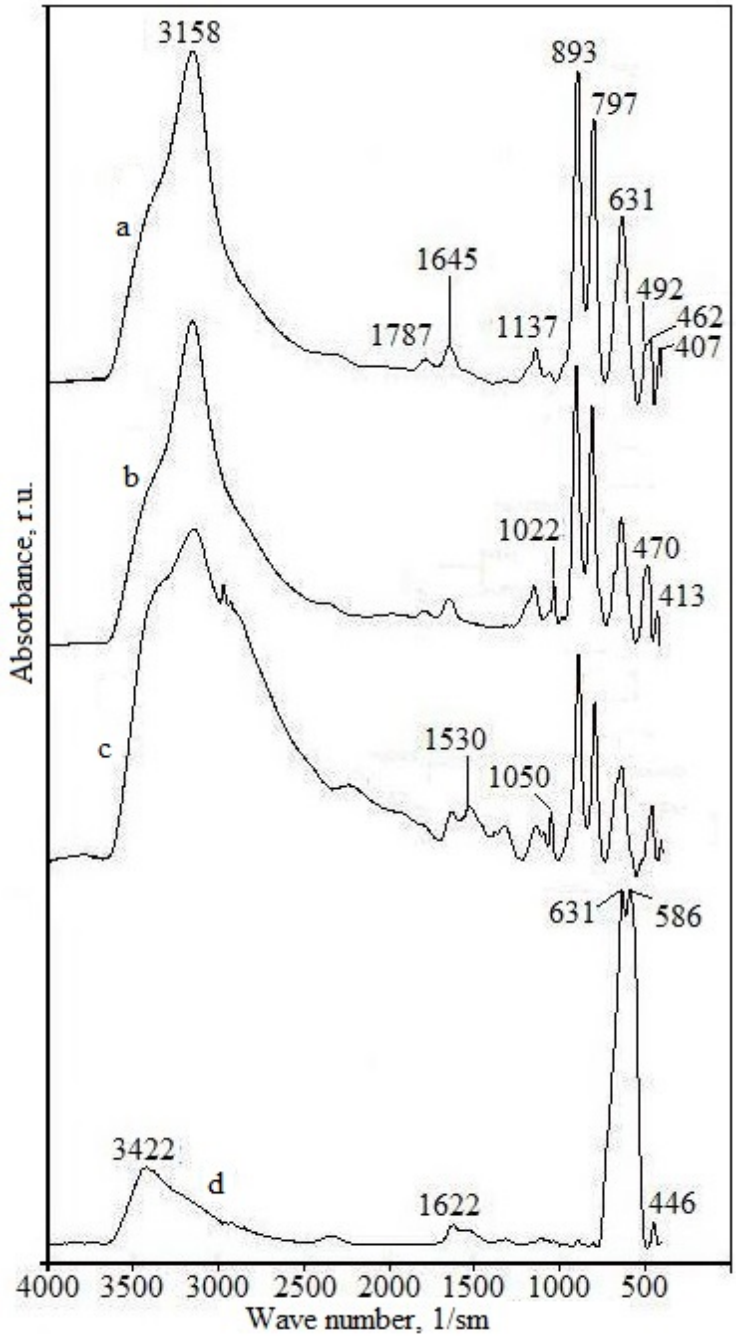

FIG. 3. The IR spectra of samples: – α-FeOOH; b – α- +γ-FeOOH; c – α- +δ-FeOOH; d – γ-Fe_2O_3.

The IR spectra of monophase samples of γ-Fe_2O_3 (Fig. 3, curve d) contain absorption bands of Fe–O bonds with wave numbers 447, 581, 626 cm^{-1}, typical of Fe_2O_3 [16], deformation vibrations of H_2O (1625 cm^{-1}), a broad absorption band with a maximum at 3441 stretching vibrations of H–O bonds and weak absorption bands of stretching vibrations of $(SO_4)^{2-}$ ions.

The thermograms for FeOOH samples are similar in many ways, therefore it is convenient to consider them on the example of thermal transformations of monophase α-FeOOH (sample 1). According to the TG data (Fig. 4), the relative mass variation in the interval 20 – 900 °C, $\Delta m_{20-900}/m_0$, for this sample is 16.49 %. On the differential thermal analysis (DTA)

curves, there are three endothermic effects with maxima at 80, 270 and 750 °C which are accompanied by reduction in mass. Mass-spectrometry studies of the gaseous phase composition revealed (Fig. 4) that the first and the second endothermic effects are due to dehydration and the third effect is caused by the decomposition of sulfate ions. According to the XPA data, at temperatures above 300 °C the α-FeOOH sample undergoes a transformation into α-Fe_2O_3. From comparison of the obtained findings with the literature data [3, 17], it can be concluded that physically adsorbed water and water of hydration (OH groups) are removed from the sample during the first and second endothermic effects, respectively. Then, the empirical structural formula FeOOH can be represented as $FeOOH(H_2O)_n(SO_3)_y$ and the thermal transformation of α-FeOOH during heatingt occurs as follows:

$$\alpha\text{-FeOOH}(\mathrm{H_2O})_\mathrm{n}(\mathrm{SO_3})_\mathrm{y} \xrightarrow{20-180\ ^\circ\mathrm{C}} \alpha\text{-FeOOH}(\mathrm{SO_3})_\mathrm{y} \xrightarrow{180-320^\circ\mathrm{C}} \xrightarrow{180-320^\circ\mathrm{C}} \alpha\text{-}\mathrm{Fe_2O_3}(\mathrm{SO_3})_\mathrm{y} \xrightarrow{>620^\circ} \alpha\text{-}\mathrm{Fe_2O_3}, \quad (1)$$

where n and y is the content of adsorbed water and $(SO_4)^{2-}$ ions in the sample expressed in terms of FeO.

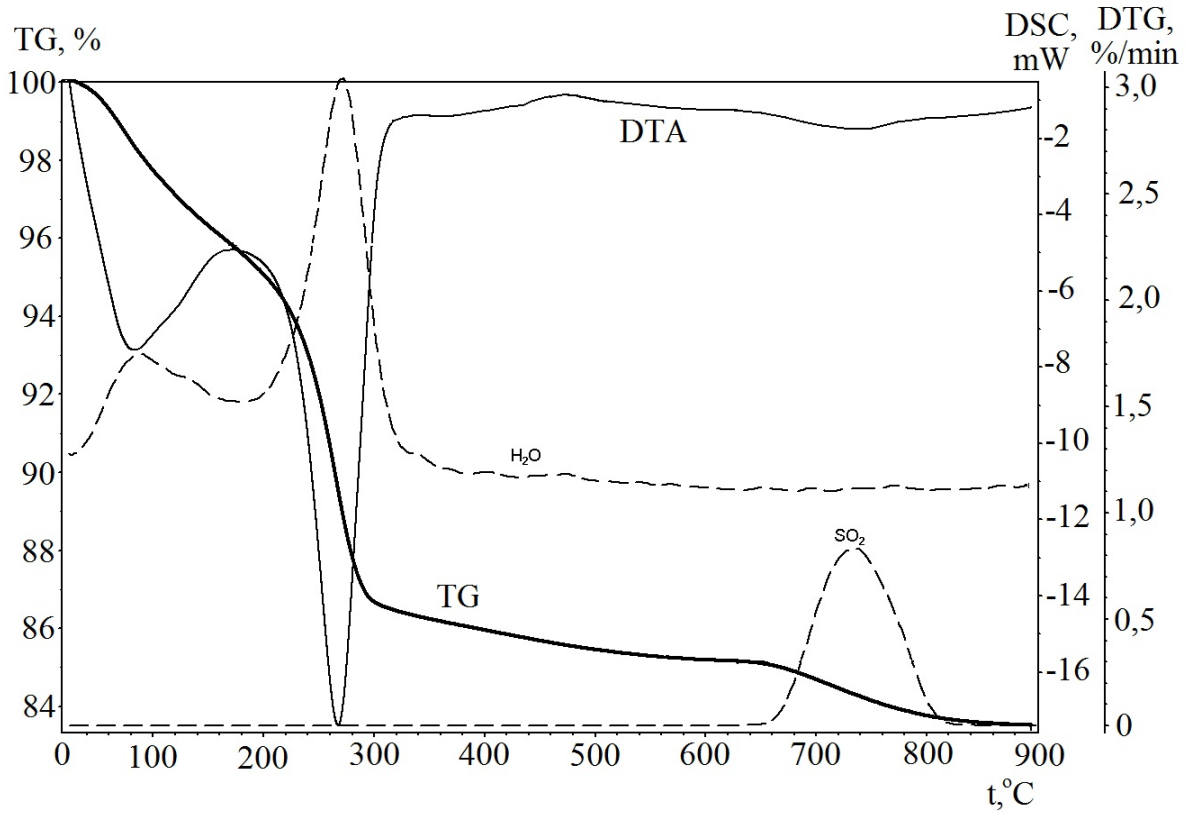

FIG. 4. The data of thermal (TG curve – heavy line, DTA curve – thin line) and mass spectrometric (H_2O, SO_2 curves – dash lines) analysis of α-FeOOH sample

From the TG data on mass variation for FeOOH samples (No. 1–4) at each stage of thermal transformation (Table 2), we calculated the values of n and y and, with allowance for the structural formula, the ratios Fe/O and S/O in the initial samples (Table 2). From Table 2, it follows that the data on the chemical composition of FeOOH samples obtained by two independent methods (XSA and TG) coincide within experiment error.

TABLE 2. Phase and chemical composition of the samples

No.	Conditions of synthesis		Phase composition	Chemical composition									
	pH	t, °C		Method PCA		Method TG							
				Fe/O, r.u.	S/O, r.u.	$\Delta m_1/m_0$[a], r.u.	$\Delta m_2/m_0$[b], r.u.	$\Delta m_3/m_0$[c], r.u.	n, r.u.	m, r.u.	y, r.u.	Fe/O [d], r.u.	S/O, r.u.
1	6.5	40	α-FeOOH[e]	0.47	0.008	0.0474	0.1011	0.0164	0.25	–	0.020	0.49	0.009
2	5.5	40	α- + γ-FeOOH	0.47	0.010	0.0444	0.1012	0.0204	0.26	–	0.024	0.48	0.010
3	6.5	20	α- + γ-FeOOH	0.46	0.014	0.0738	0.1011	0.0297	0.24	–	0.038	0.47	0.015
4	13.0	40	α- + δ-FeOOH	0.52	0.001	0.0407	0.1011	–	0.21	–	< 0.001	0.50	–
5	6.5	85	γ-Fe_2O_3[f]	0.57	0.004	0.021	0.0168	0.0042	0.195	0.156	0.009	0.63	0.003
6	10.5	40	γ-Fe_2O_3	0.50	0.002	0.0194	0.0155	0.0021	0.179	0.143	0.0044	0.63	0.0015

a) $\Delta m_1/m_0$ – relative mass loss of the sample at the temperature(20 – 180 °C, 1st end of thermic effect);
b) $\Delta m_2/m_0$ – relative mass loss of the sample at the temperature (200 – 500 °C, 2nd end of thermic effect);
c) $\Delta m_3/m_0$ – relative mass loss of the sample at the temperature 500 – 900°C;
d) we didn't tack into consideration amount of oxygen, participated in the samples in the form of adsorbed water due to total desorption of this form of water molecules in the high vacuum chamber of the PCA analytical installation used.
e) empirical formula of the α-, γ-, δ-FeOOH contained samples is $FeOOH \cdot nH_2O \cdot SO_3$.
f) empirical formula of the Fe_2O_3 contained samples is $Fe_2O_3 \cdot (n + m)H_2O \cdot ySO$.

The DTA curves of monophase samples of γ-Fe_2O_3 (Fig. 5) have two endothermic effects with maxima at 80 and 260 °C which are due to removal of physically adsorbed water and water of hydration and are accompanied by mass loss. Also present is a pronounced exothermic effect at 560 °C, occurring without any noticeable variation in the sample mass (the mass reduction from 500 – 900 °C is $\sim$ 0.2 %). The XPA data show that the exothermic effect is brought about by the phase transition of γ-Fe_2O_3 into α-Fe_2O_3. Assuming that the variation of the mass for the Fe_2O_3 samples at temperatures above 500 °C, as in the case of FeOOH, is caused by the process of desulfation, the structural formula of Fe_2O_3 can be represented as $Fe_2O_3(H_2O)_n(SO_3)_y$ and its thermal transformation during heating occurs in the following manner:

$$\begin{gathered}\gamma\text{-}Fe_2O_3(H_2O)_{(n+m)}(SO_3)_y \xrightarrow{20-180^\circ C} \gamma\text{-}Fe_2O_3(H_2O)_m(SO_3)_y \xrightarrow{180-500^\circ C} \\ \xrightarrow{180-500^\circ C} \gamma\text{-}Fe_2O_3(SO_3)_y \xrightarrow{500-900^\circ C} \alpha\text{-}Fe_2O_3,\end{gathered} \tag{2}$$

where n, m and y are the contents of adsorbed water and water of hydration and $(SO_4)^{2-}$ ions in the sample expressed in terms of Fe_2O_3.

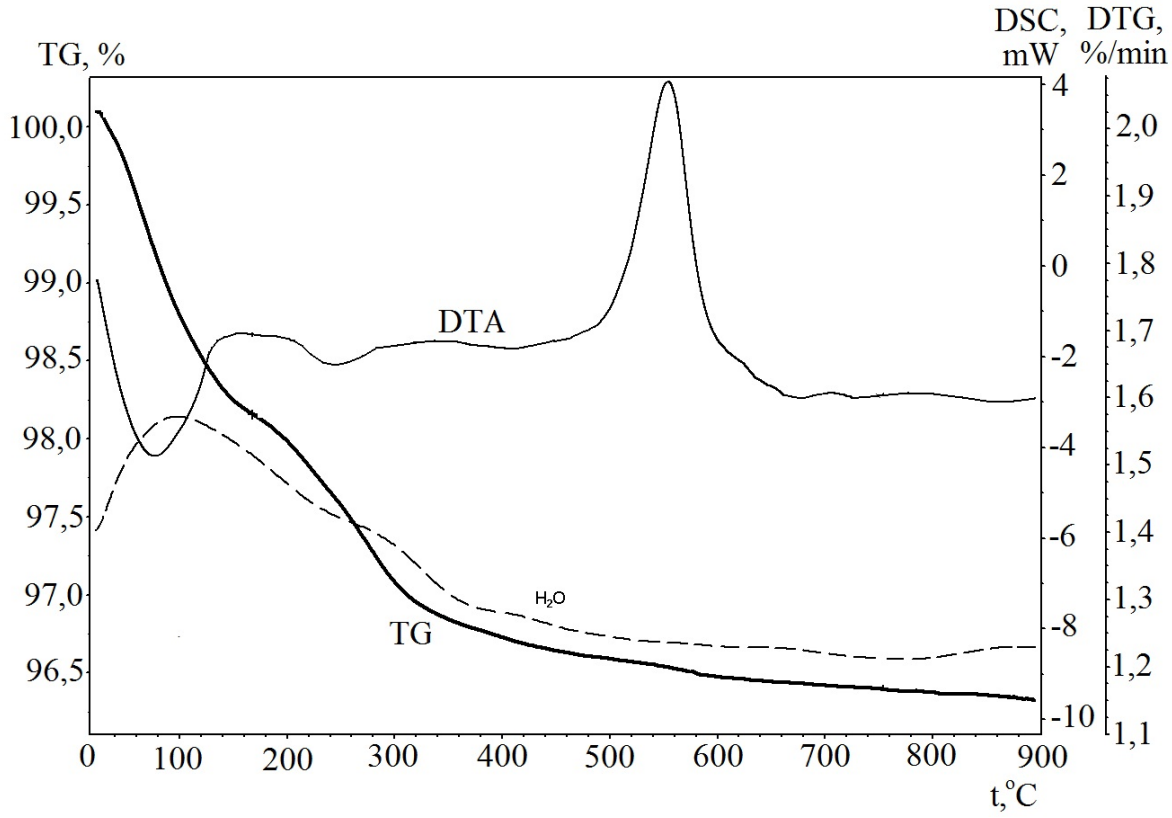

FIG. 5. The data of thermal (TG curve – heavy line, DTA curve – thin line) and mass spectrometric (H_2O curve – dash line) analysis of γ-Fe_2O_3 sample

As in the case of thermal transformations of FeOOH, values for m, n and y were calculated from the TG data, and the ratios Fe/O and S/O in the initial samples were determined taking into account the structural formula (Table 2). From Table 2, it follows that the XSA method gives a slightly underestimated Fe/O ratio in the γ-Fe_2O_3 samples as compared to TG analysis.

The established dependence of the phase and disperse compositions of the precipitates formed in the $FeSO_4$ – H_2O – KOH – H_2O_2 system on the oxidation parameters agrees on the whole with the results obtained from the examination of analogous systems [2, 3, 6–12] and provides evidence that crystal growth during the oxidation of aqueous solutions of iron(II) salts and (or) suspensions of iron(II) hydroxide, especially at low temperatures, takes place under conditions of high supersaturation. As a result, the average size of crystals decreases, their imperfections increase, and phases with disordered crystal structure are formed, in particular, δ-FeOOH. At the same time, it should be noted that our data for γ-Fe_2O_3 phase formation do not agree with previous results [7, 18] for the formation of the Fe_3O_4 phase during the oxidation of $Fe(OH)_2$ suspensions by atmospheric air under analogous conditions (pH $\approx$ 9). This contradiction is eliminated if we assume that in our experiments the application of a more active oxidizer (H_2O_2) originally leads to the formation of the Fe_3O_4 phase in a nanodisperse state, which is subsequently oxidized by hydrogen peroxide to γ-Fe_2O_3 by a topotactical solid-state reaction mechanism. The possibility of $Fe_3O_4 \rightarrow \gamma$-$Fe_2O_3$ transformation occurring in oxygen-containing aqueous media has been reported previously [3, 19].

The synthetic conditions for oxyhydroxide phases in the examined system are characterized by high supersaturaion and lead to the formation of nanodisperse primary particles, which, owing to developed specific surface area, are apt to form compact aggregates, whose average size (D) increases as d decreases [3]. In this connection, it is interesting to consider the empirical dependence between the size of primary crystals of new phases and the temperature of synthesis in the framework of the familiar nucleation model [20]. From this dependence, it follows that the relation between the average size of primary crystals d (nm) of phases formed in the $FeSO_4$ – KOH – H_2O – H_2O_2 system at a fixed value and temperature (Fig. 2 and Table 1) obeys the Kelvin equation:

$$\mathrm{R}T\ln(a/a_0) = 4\gamma\overline{V}/d, \tag{3}$$

in which the average size of primary crystals (d) correlates with their relative solubility; a, a_0 is the solubility of crystals of size d under synthetic conditions and of crystals with infinitely large size under equilibrium conditions; γ, $\overline{V}$ is the interfacial tension determining the solubility and molar volume of crystal; R is the universal gaseous constant; and T is the temperature of formation for crystals of a given size [20]. Then, we transform equation (3) to a form convenient for the analysis of experimental dependences (4) by the least square method:

$$1/d = b[0] + b[1]T, \tag{4}$$

where $b[0]$ is the empirical constant and $b[1] = R\ln(a/a_0)/4\gamma\overline{V}$. It is seen that all the empirical data on the sizes of primary crystals and the synthesis temperature for the $FeSO_4$ – KOH – H_2O – H_2O_2 system obey equation (4). In Fig. 6, these experimental dependences are represented in the coordinates of equation (4) and are characterized by the correlation coefficient in the range (0.94 – 0.99) and by the Fisher F-criterion parameter for the nucleation model (50 – 120). A peculiar feature of Fig. 6 is a negative value for the parameter $b[1]$ in eq. (4). This may imply that $\ln(a/a_0) < 0$ or the relative solubility of primary crystals during synthesis is $(a/a_0) < 1$. This dependence contradicts the model of critical nucleus formation both during the condensation of liquid drops from vapor and during primary particle crystallization from aqueous solutions of electrolytes [20] and can be explained by the fact that the majority of primary particles inside the compact aggregates are isolated from the mother solution and do not affect the value of a_0, while the contribution to the solubility of new phase is made mainly by the small crystals located on the surface of aggregates. Indeed, from Fig. 7, it is seen that the growth of primary crystal sizes and consequently the reduction of the average aggregate size D

results in the disappearance of anomalous relative solubility when the particle size approaches 25 – 35 nm, whereas further increase in the primary particle sizes with the growth of d may lead to a traditional character of temperature dependence for therelative solubility, $(a/a_0) > 1$.

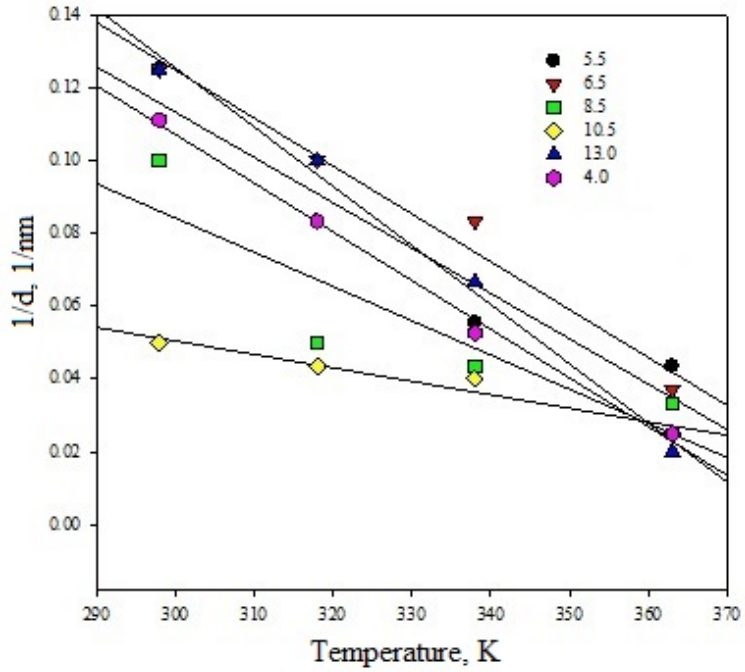

FIG. 6. The average crystal size d (nm) of phases formed in the system $FeSO_4$ – KOH – H_2O – H_2O_2 at a fixed pH value as a function of temperature represented in the coordinates of equation (4). Inset: the synthesis pH values are designated by figures.

In conclusion, let us consider the nature of the water of hdration in γ-Fe_2O_3. According to [9, 19, 21], the nanodisperse samples of γ-Fe_2O_3, as distinct from coarse crystalline ones, have a spinel-type defect structure and regular defects in the cationic sublattice. The structural formula of nanodisperse γ-Fe_2O_3 is $Fe_8\square_{2.67}Fe_{13.33}O_{32}$, where $\square$ is a vacancy in the octahedral cationic positions. In the topochemical oxidation reaction, water molecules of the solution can occupy the vacant positions, forming hydrogen bonds with oxygen anions and thereby stabilize the γ-Fe_2O_3 lattice. This explains the higher temperatures for removing the water of hydration on the thermograms of γ-Fe_2O_3 (above 200 °C) as compared to adsorbed water.

4. Conclusion

For wide temperature (20 – 85 °C) and (4.0 – 13.0) intervals of the reaction medium, we have established the regularities for the formation of nanodisperse iron(III) oxide compounds during the oxidation of aqueous $FeSO_4$ solutions and (or) $Fe(OH)_2$ suspensions by hydrogen peroxide under quasi-stationary conditions with the use of KOH as an alkaline agent. The dependences of the phase, chemical and disperse compositions of the resulting products upon the synthetic conditions have been determined.

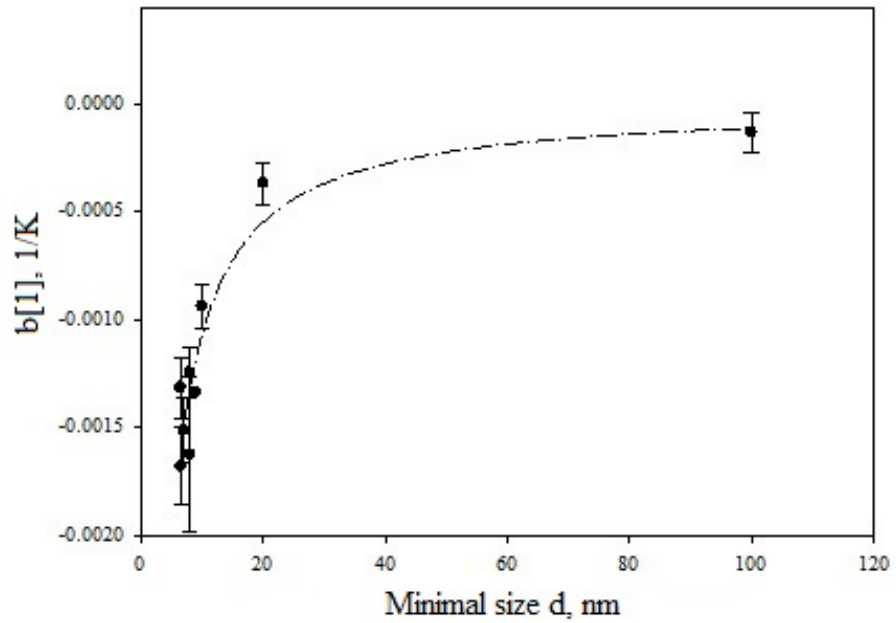

FIG. 7. The variation of the inclination angle $b[1]$ in the empirical equation (4) as a function of the minimal size of primary crystals registered in each series of experiments at constant pH in the system $FeSO_4$ – KOH – H_2O – H_2O_2. The line in the Figure exhibits a tendency towards $b[1]$ variation with the growth of the size of primary particles.

References

[1] Bharat B. *Handbook of Nanotechnology*. Springer-Verlag Heidelberg, Berlin, 2010, 1961 p.

[2] Cornell R.M. Schwertmann U. *The iron oxides. Structure, properties, reactions, occurrences and uses*. WILEY-VCH Verlag GmbH & Co. KGaA, Weinheim, 2003, 694 p.

[3] Kleschev D.G., Sheinkman .I., Pletnev R.N. *The effect of medium on the phase and chemical transformations in disperse systems*. UrO AN SSSR, Sverdlovsk, 1990, 248 p. [in Russian]

[4] Polyakov E.V., Krasilnikov V.N., et al. Synthesis and photocatalytic activity of quasi-one-dimensional (1-D) solid solutions $Ti_{1-x}M_xO_{2-2x/2}$ (M(III)= Fe(III), Ce(III), Er(III), Tb(III), Eu(III), Nd(III and Sm(III), $0 \leq x \leq 0.1$)). *Nanosystems: physics, chemistry, mathematics*, 2014, **5** (4), P. 553–563.

[5] Mallikarjuna N.N., Manohar S.K., et al. Novel high dielectric constant nanocomposites of polyaniline dispersed with γ-Fe_2O_3 nanoparticles. *J. Appl. Polym. Sci.*, 2005, **97** (5), P. 1868–1874.

[6] Feitknecht W. Uber die Oxydation von festen Hydroxyverbindungen des Eisens in wabbrigen Losungen. *Zs. Elektrochem*, 1959, **63** (1), P. 34–43.

[7] Kijama M. Conditions for the formation of Fe_3O_4 by the air oxidation of $Fe(OH)_2$ suspensions. *Bull. Chem. Soc. Japan.*, 1974, **47** (7), P. 1646–1650.

[8] Misawa T., Hashimoto K., Shimodaria S. The mechanism of formation of iron oxides and oxihydroxides in aqueous solutions at room temperatures. *Crrsion Sci.*, 1974, **4** (2), P. 131–149.

[9] Datta N.C. Chemistry of iron(III) oxides and oxyhydroxide. *J. Sci. Industr. Res.*, 1981, **40** (9), P. 571–583.

[10] Kijama M., Takada T. Iron compounds formed by the aerial oxidation of ferrous salt solutions. *Bull. Chem. Soc. Japan.*, 1972, **45** (10), P. 1923–1924.

[11] Tolchev A.V., Kleschev D.G., Bagautdinova R.R., Pervushin V.Yu. Temperature and pH effect on composition precipitate formed in $FeSO_4$ – H_2O – H^+/OH^- – H_2O_2 system. *Mat. Chem. Phys.*, 2002, **74** (1), P. 336–339.

[12] Inouye K. What is Iron Oxyhydroxide. *Kagaku to Kogyo*, 1974, **27** (8), P. 571–578.

[13] Weckler B., Lutz H.D. Lattice vibration spectra. Part XCV. Infrared spectroscopic studies on the iron oxide hydroxides goethite (α), akaganeite (β), lepidocrocite (γ), and feroxyhite (δ). *Eur. J. Solid State Inorg. Chem.*, 1998, **35** (8–9), P. 531–544.

[14] Nakamoto K. *Infrared and Raman Spectra of Inorganic and Coordination Compounds*. Sixth edition. WILEY: A John Wiley & Sons, Inc., Publication. Hoboken, New Jersey. 2009, 427 p.

[15] Weckler B., Lutz H.D. IR spectroscopic studies on iron oxide hydroxides. *Eur. J. Solid state Inorg. Chem.*, 1998, **35**, P. 531–544.

[16] Sidhu P.S. Transformation of trace element-substituted maghemite to hematite. *Clays and Clay Minerals*, 1988, **36** (1), P. 31–38.

[17] Koga N., Takamoto Sh., Okada S., Tanaka H. A kinetic study of the thermal decomposition of iron(III) hydroxide oxides. Part 1. α-FeOOH in banded iron formatins. *Thermochimica Acta*, 1995, **254** (1), P. 193–206.

[18] Kleshcheva R.R., Kleshchev D.G., et al. The effect of synthesis parameters on the phase formation in the system $FeSO_4$ – H_2O – H^+/OH^- – O_2 ($3.5 \leq$pH ≤ 13). *Russian Journal of Applied Chemistry*, 2003, **76** (9), P. 1379–1383.

[19] Gallagher K.S., Feitknecht W., Mannweiler U. Mechanism of oxidation of magnetite to γ-Fe_2O_3. *Nature*, 1968, **127** (5134), P. 1118–1121.

[20] Adamson A.W., Gast A.P. *Physical chemistry of surface*. Sixth edition. A WILEY-INTERSCIENCE PUBLICATION: A John Wiley & Sons, Inc. 1997, 804 p.

[21] Bernal J.D., Dasgypta D.R., Mackay A.S. The oxides and hydroxides of iron and their structural interrelationships. *Clay miner. Bull.*, 1959, **4** (2), P. 131–149.